Scientific African 23 (2024) e02007

Contents lists available at ScienceDirect

Scientific African

journal homepage: www.elsevier.com/locate/sciaf

FaceNet recognition algorithm subject to multiple constraints: Assessment of the performance

Joseph A. Mensah [a], Justice K. Appati [c], Elijah K.A Boateng [a], Eric Ocran [b], Louis Asiedu [b,*]

[a] Department of Computer Science, Ashesi University, No. 1 University Avenue, Berekuso, Eastern Region, Ghana
[b] Department of Statistics and Actuarial Science, College of Basic and Applied Sciences, University of Ghana, Ghana
[c] Department of Computer Science, College of Basic and Applied Sciences, University of Ghana, Ghana

ARTICLE INFO

Editor name: Aboul Ella Hassanien

Keywords:
FaceNet algorithm
MICE
MissForest
RegEM
Occlusion
Varying expressions
Augmentation schemes

ABSTRACT

Literature has it that the performance of most face recognition algorithms still decline in multiple constrained environments (Occlusions and Expressions), despite the achieved successes of deep learning face recognition algorithms. Using expression variant test face images synthetically occluded at 30% and 40% rates, the study evaluated the performance of FaceNet deep learning model for face recognition under the aforementioned constraints and when three (3) statistical multiple imputation methods (Multivariable Imputation using Chain Equations (MICE), MissForest and Regularized Expectation Maximization (RegEM)) are adopted for occlusion recovery. Results of the study showed improved recognition rates of the study algorithm when the imputation-based recovered faces were used for recognition compared with using their multiple constrained counterparts. However, test faces reconstructed with the MissForest imputation method were more accurately recognized using the FaceNet deep learning algorithm. Furthermore, the study demonstrated that some simple augmentation schemes sufficed to further enhance the performance of the FaceNet model. Specifically, the FaceNet algorithms gave the highest average recognition rates (85.19% and 79.5% for 30% and 40% occlusion levels respectively) under augmentation scheme IV (slight rotations, horizontal flipping, shearing, brightness adjustments, and stretching) using MissForest as the de-occlusion mechanism. The study also found that, no disparity existed in its performance with the choice of either Support Vector Machines (SVM) or City Block (CB) for classification under augmentation scheme IV. The study recommends using the MissForest imputation method in dealing with moderately high occluded test faces with varying expressions to enhance the performance of the FaceNet face recognition model.

Introduction

Knowing the identity of unknown people is crucial in most jurisdictions, particularly among humans, to establish communication, promote peaceful coexistence, gain access to necessary services, and safeguard lives and property. Modern times have seen recognition technologies based on biometric information to speed up the procedure. It is typically necessary for facial recognition systems to be trained to identify unfamiliar faces using photographs of people. However, the problem of limited images for training as well as the prevalence of inimical environmental factors and constraints (eg. expressions, lighting, occlusions, head-tilt or poses,

* Corresponding author.
E-mail address: lasiedu@ug.edu.gh (L. Asiedu).

https://doi.org/10.1016/j.sciaf.2023.e02007
Received 24 August 2023; Received in revised form 13 November 2023; Accepted 29 November 2023
Available online 6 December 2023

ageing etc.) continue to hamper the performance of even the best-performing algorithms [1,2]. It is known that the performance of face recognition algorithms generally decline when trained on images acquired under particular environmental constraints but are tested on images acquired under different environmental constraints. Some studies [3,4] have reported that when recognition involves matching features selected from train-image databases containing only the neutral-expression face images of subjects with that of test faces acquired under non-neutral expressions (eg, angry, sad, disgust, fear, happy), the recognition rates are often poorer. This, according to Goren and Wilson [5], could be due to the magnitude of geometric dissimilarity between the train and test face images. Also, these constraints acts as noise and hence degrade the image quality. Multiple constrained environment is defined as the presence of more than one constraint (either expression, occlusion, lighting, head-tilt or pose, ageing, etc.). An image is said to be acquired under multiple constraints when more than one of the above listed constraints exist during the image acquisition. In this study, the constraints under consideration are occlusions and expressions. Alyüz et al. [6] and Lahasan et al. [7] details how occlusions account for the poor performance of many automatic face recognition systems . As underscored in [8], the presence of occlusions could block access to facial features, rendering a more degraded version of the real image of the subject. Occlusions could also corrupt the pixels in the acquired images and as well affect their distribution and any facial embeddings thereof. To deal with the occlusion challenge in test faces, considerable amounts of efforts have focused on pre-training algorithms with images obtained under similar constraints. However, the universality of this approach is debatable, as in most instances the success of this approach may be contingent on the availability of such training datasets, which is often limited. Therefore, the search for face recognition systems that are invariant to the presence of occlusions or those that might require some form of image enhancements to improve their performance continue to be central to ongoing research works in automatic face recognition. Image reconstruction or restoration is one such method.

Image reconstruction techniques could be broadly classified as machine learning-based or Statistical (model) based. The former class of methods attempts to reconstruct an image by generating a data model from the dataset with missing values and then using the model to perform classification that imputes the missing values [9]. This class of methods are known to be fast but have sub-optimal properties such as poor resolution-noise tradeoff for some class of images. Besides, they are characterized by complex architectures [10]. The model-based reconstruction methods, on the other hand, iteratively obtain estimates of the missing pixels in a degraded image based on statistical model(s) [11]. They assume that the population of image pixel values are realizations of random variables, characterized by unknown population parameters (and therefore perform parameter estimation), together with assumed prior information about the underlying unknown image such as smoothness, or sparsity in a transformed domain. These iterative methods are known to improve image quality by reducing noise and artefacts [12,13]. Although there is some evidence to show that the Multivariate Imputation with Chain Equations (MICE) could enhance the performance (recognition distances) of Principal Component Analysis (PCA) recognition algorithms, under low levels of random occlusions [14], to the best of our knowledge, no prior works have investigated the effects of using statistical multiple imputation schemes for occlusion recovery on the performance of the FaceNet deep learning face recognition model when moderately high occlusions and varying expressions are the underlying constraints.

Using algorithms in research is essential because they allow for the systematic and practical completion of complex tasks, data analysis, and problem-solving. Algorithms also allow research to be replicated since they can be recorded and shared with others, aiding in confirming the accuracy and reliability of results [15]. Deep learning-based models or algorithms often involve the use of artificial neural networks comprising several layers [16]. In deep learning, non-linear transformations and model abstractions of high levels are applied to large databases [17]. Deep learning has been widely applied in areas such as image super-resolution, inpainting, decolorization and characterization [18], Medicine [19–22], Biometrics [23] and handwritten character recognition [24]. FaceNet is a pre-trained deep learning algorithm developed by Google [25]. FaceNet directly learns a mapping from face images to a compact Euclidean space where distances directly correspond to a measure of face similarity [25]. One of its advantages is its ability to allow one to extract high-quality features from faces called face embeddings that can be used to train face identification systems [26]. Applications of FaceNet includes real-time web-based face recognition systems for detecting faces [27], early fatigue detection while working at the computer and real-time masked face recognition [28]. The performance of the FaceNet model has been reported by some authors in literature. In [27], the authors implemented a real-time web-based face recognition system. They compared three different face recognition modules (FaceNet-SVM, PCA-SVM, K-NN). The results indicated that the FaceNet-SVM recognition module attained the highest accuracy on three different datasets. In [28], the authors demonstrated that combining FaceNet with K Nearest Neighborhood (KNN) classification improved the accuracy compared with using multiclass Support Vector Machine (SVM) for classification (94.66% and 89.87% respectively). However, combining FaceNet with multiclass SVM attained a relatively lower runtime. The authors Adhinata et al. [29] investigated the use of FaceNet with three classifiers (SVM, K-NN, Random Forests) in a real-time masked face recognition problem. Their results showed that FaceNet with Random Forests attained the least accuracy (54.04%) while FaceNet with multi-class SVM attained the highest accuracy (96.15%). However, all three FaceNet modules had a relatively similar runtime. In other works, Golla and Sharma [30] evaluated the performance of FaceNet on low resolution face images compared to high resolution face images.

Despite the high performance of the FaceNet model as reported in existing works, little is known about its performance under multiple constraints (the presence of moderately high levels of occlusions (30% & 40%) in test faces also acquired under varying expressions), especially when one image per subject is available for training. The use of statistical multiple imputation-based reconstructed faces in deep learning face recognition tasks is particularly crucial, not only to evaluate the efficacy of reconstruction, but also to assess the relative merits of their use with deep learning face recognition models. This study, therefore, seeks to assess the performance of the FaceNet model in the presence of multiple constraints and the relative merits of using different statistical multiple imputation schemes on its performance, with and without train image data augmentation where there is only a limited

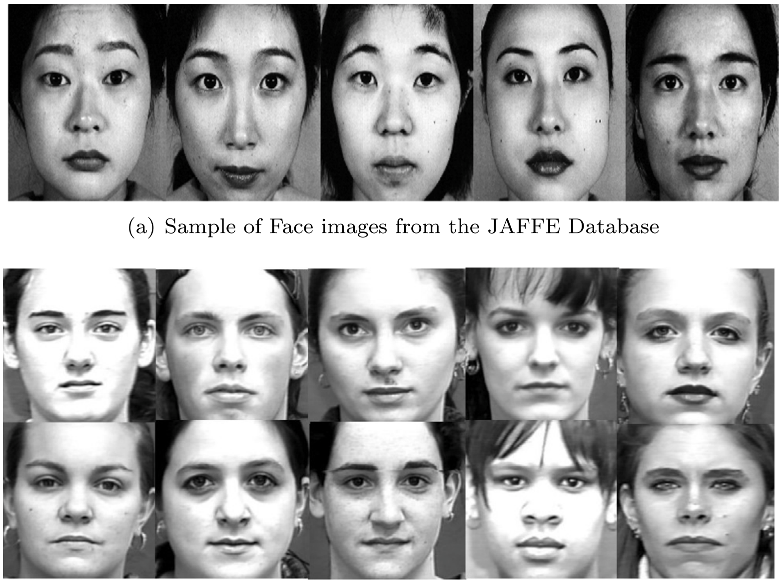

(a) Sample of Face images from the JAFFE Database

(b) Sample of face images from the Cohn-Kanade Database

Fig. 1. Sample of faces of subjects in the train-image database.

number of images per subject for training. The main performance assessment metrics would be the average recognition rate and the run-time or computational time of the study algorithm.

The remaining parts of the paper are arranged as follows: The Methods and Material section contains a description of acquired data and the methods used for the study. The section also presents the de-occlusion methods and the augmentation schemes considered in the study. The Results and Discussion section contains the performance assessment results of the study algorithm across the various augmentation schemes and de-occlusion mechanisms. The conclusion section summarizes the findings and provides directions for future research.

Methods and materials

Data acquisition

Databases: The Japanese Female Facial Expression (JAFFE) and the AU-Coded Cohn–Kanade (CKFE) databases were used to benchmark the performance of the study recognition algorithms.

- Train-image database: This contains the neutral expression faces of 36 subjects (10 from JAFFE and 26 from CKFE databases). These images will serve as a basis for six (6) train-image data augmentation schemes in Section "Train Image Data Augmentation Schemes". A sample of subjects in the train-image database is presented in Fig. 1.
- Test-image databases: The expression variant (angry, disgust, fear, happy, sad, surprise) faces of the 36 subjects in the train-image database were synthetically occluded randomly to create 30% and 40% missingness in the faces' pixels. The resultant images were, thus, characterized by both varying occlusions and expressions and hereafter referred to as multiple constrained test faces. Fig. 2 depicts a sample of the multiple constrained face images. These multiple constrained faces were subsequently reconstructed using the MICE, MissForest and RegEM multiple imputation methods and the resultant images were captured into separate test-image databases.

Reconstruction mechanisms

One of the main factors that affect the performance of face recognition algorithms is the presence of degradations and noise in acquired or processed images [31]. As such, enhancing the quality of face images may suffice to improve the performance of recognition algorithms. Three statistical multiple imputation methods were adopted in an attempt to reconstruct missing facial information due to the 30% and 40% synthetic occlusion rate in the expression variant test faces.

(a) Sample of 30% Synthetically occluded images (Happy expression)

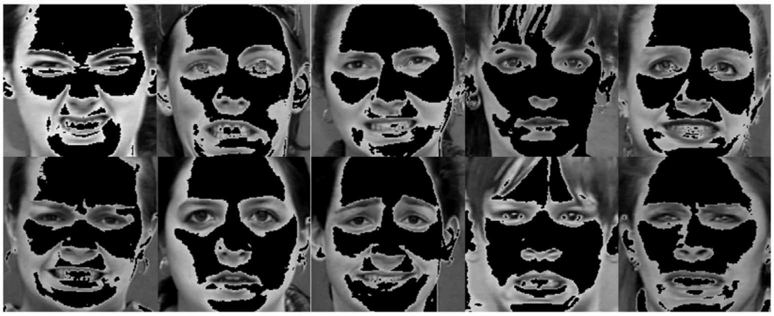

(b) Sample of 40% Synthetically occluded images (Sad expression)

Fig. 2. Synthetically occluded faces.

Regularized expectation maximization (RegEM)

Owing to the fact that the noise in pixel intensities of a face image is Gaussian [32] and the image matrix representation corresponding to an occluded face is under-sampled, it is natural to consider the reconstruction problem as an optimization problem in which a regularized least-squares cost function is minimized [11]. The Regularized EM reconstruction casts the image reconstruction problem as an optimization problem as follows:

$$\hat{x} = \arg\min\ x g(x) + \beta R(x), \tag{1}$$

where, x is an unknown face image, $g(x)$ is a data-fidelity term (least-squares cost function), $R(x)$ is a regularizer that forces the reconstructed image $\hat{x}$ to have some assumed prior properties such as smoothness or sparsity in a transformed domain (eg. wavelet, Fourier) and β is a regularization parameter that controls the trade-off between over-fitting the (noisy) image data and sparsity or over-smoothing the image. Since face images are naturally "near sparse", $L2$ regularization was performed, and the regularization parameter was chosen by the method of cross-validation [33]. Refer to the works of Liu and Brown [34], Le et al. [35], Liang et al. [36] and Liu et al. [37] for detailed information about the regularized expectation maximization (RegEM) algorithm and its applications.

Multivariate Imputation by Chain Equations (MICE)

The MICE multiple imputation method is a flexible parametric imputation method [38]. As such it has been used to handle missing data in diverse domains of study [39]. The MICE algorithm operates on the assumption that the probability of a data missing may depend on the observed values (Missingness mechanism is Missing at Random (MAR)). For each variable (column) with missing data, the MICE multiple imputation algorithm iteratively imputes missing values as random draws from the conditional distribution of the variable, given all other variables [40] as follows:

1. Perform variable mean imputation for each variable (column) with missing pixel intensities.
2. Starting with a column X in the occluded face image with missing pixel intensities, regress X on all other columns other than X to obtain the parameters of the regression model.
3. Using the regression model, with the model parameters calculated (in step 2), obtain new random estimates of the missing values in X and replace the former estimates accordingly.
4. Repeat steps 2 and 3 for all columns with missing intensities.
5. Iterate through steps 2 and 3 until convergence or for a specified number of iterations.

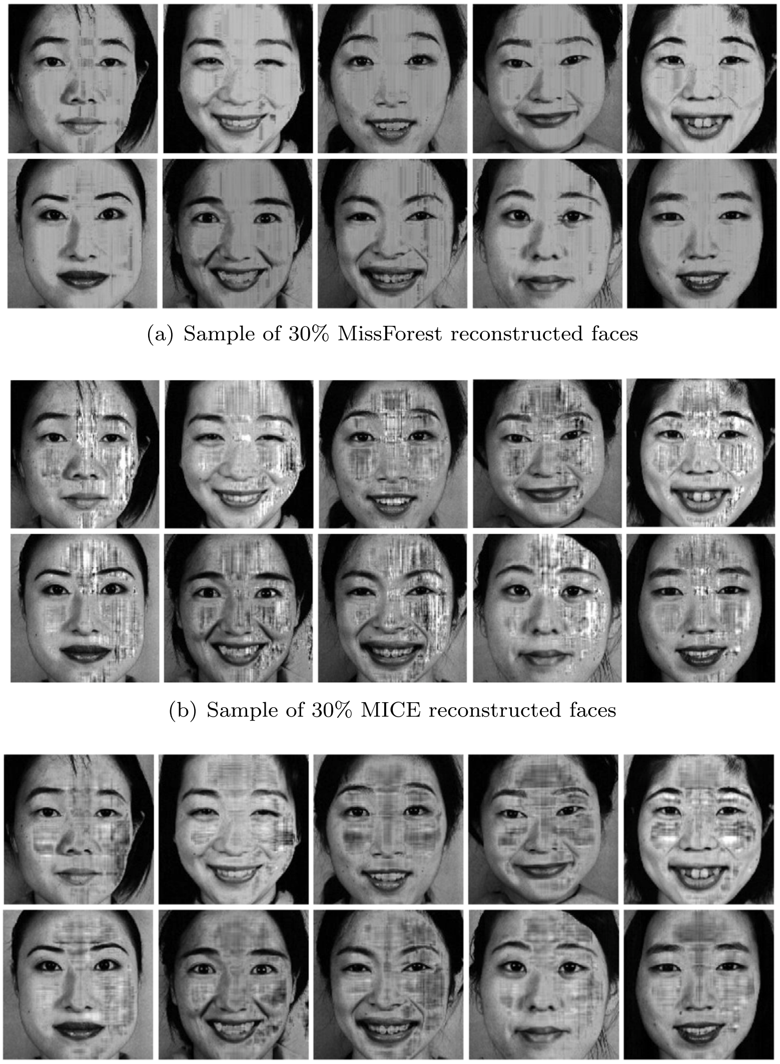

(a) Sample of 30% MissForest reconstructed faces

(b) Sample of 30% MICE reconstructed faces

(c) Sample of 30% RegEM reconstructed faces

Fig. 3. Sample of 30% reconstructed faces.

In this work a maximum of 10 iterations were carried out during the reconstruction process. The following Resche-Rigon et al. [41], Hughes et al. [42] and Resche-Rigon and White [43] are some notable works about Multivariate Imputation by Chain Equations (MICE) algorithm and its application in literature.

MissForest

Research into Random forest-based imputation models are becoming increasingly popular in diverse fields of study [44]. The MissForest imputation algorithm is one of such machine learning-based algorithms that is known to handle mixed-type of data (continuous and categorical), non-linearities as well as complex interactions in data without requiring any distributional assumptions about the variables [45]. This notwithstanding, the imputation ability of MissForest still remains inconclusive in literature, as mixed performances have been reported by several authors [46–48]. The MissForest imputation method works sequentially as the MICE, but instead creates random forest models for each variable with missing pixels and generates predictions from such models [45].

Figs. 3 and 4 show some sample multiple imputation based reconstructed expression faces at 30% and 40% occlusion rates respectively.

Train image data augmentation schemes

Data augmentation mechanisms have been proposed as a viable approach to increasing the number of images for pre-training algorithms in the case of limited training data [49]. These augmentations may comprise one or several variations of the subjects in

(a) Sample of 40% MissForest reconstructed faces

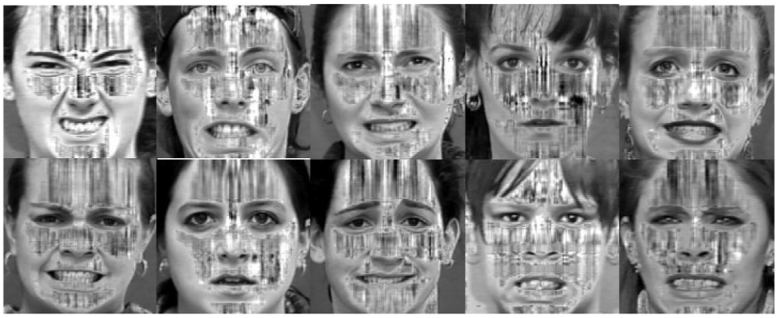

(b) Sample of 40% MICE reconstructed faces

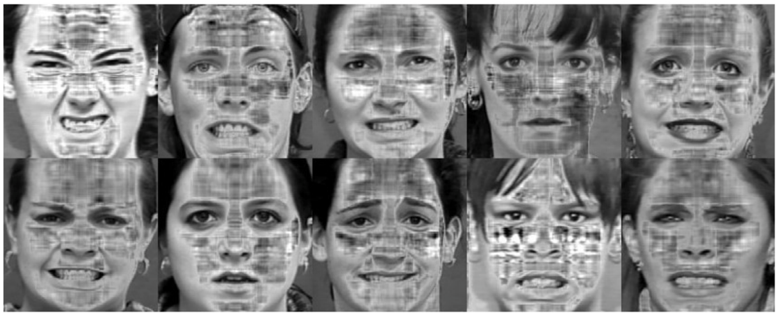

(c) Sample of 40% RegEM reconstructed faces

Fig. 4. Sample of 40% reconstructed faces.

the training datasets. Six (6) augmentation schemes were explored in an attempt to enhance the performance of the study recognition algorithm.

Augmentation using left reconstructed faces (Scheme I)

The first (Scheme I) augmentation scheme comprised augmenting the neutral image of each subject in the train-image database with their respective left half reconstructed face.

The left half-face images obtained by vertical segmentation of the neutral images of subjects are reconstructed as follows:

i. Denote the left segmented neutral half-face as H_{L1}.
ii. Transpose the left segmented half image followed by a rotation of the resultant image through 90 degrees in the clockwise direction and denote it as H_{L2}.
iii. Concatenate H_{L1} and H_{L2} as

$$T_L = \left[H_{L1}|H_{L2}\right]. \tag{2}$$

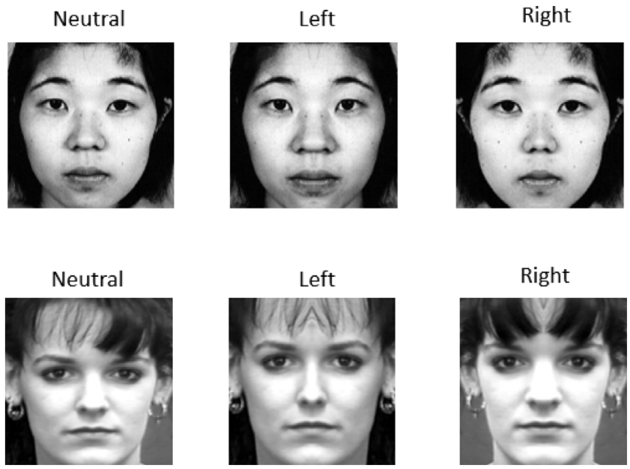

Fig. 5. Sample images of two subjects in augmentation schemes I and II.

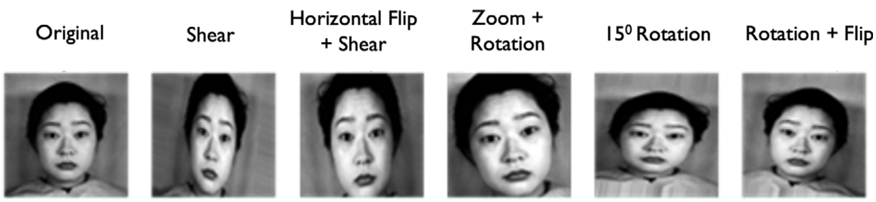

Fig. 6. Sample images of a subject obtained using augmentation scheme IV.

Augmentation using right reconstructed faces (Scheme II)

The second (Scheme II) augmentation scheme comprised augmenting the neutral image of each subject with their respective right reconstructed images created from half segmentation of the neutral images. The right half-face images acquired are reconstructed as follows:

i. Denote the right segmented neutral half image as H_{R1}.
ii. Rotate the right segmented half image 90 degrees in the anticlockwise direction and transpose the resultant image and denote it as H_{R2}.
iii. Concatenate H_{R2} and H_{R1} as

$$T_R = \left[H_{R1} | H_{R2} \right]. \tag{3}$$

Augmentation schemes I and II were motivated by the study of the authors in [32] who demonstrated that left and right reconstructed faces may be suitable to recognize frontal faces in PCA-based face recognition under partial (half) occlusion constraints, although in their case they explored their use as test faces. Fig. 5 shows the left and right reconstructed faces of two subjects with neutral expression as used in augmentation schemes I and II.

Augmentation using both left and right reconstructed faces (Scheme III)

This augmentation scheme combined schemes I and II. Thus, both left and right reconstructed face images of each subject were used for augmentation.

Augmentation Scheme IV

This augmentation scheme sought to incorporate five additional face images per subject to their neutral faces. This augmentation approach involved applying various transformations, including slight rotations, horizontal flipping, shearing, brightness adjustments, and stretching. Each of the five augmented images combined up to two of these parameters. Fig. 6 shows images emanating from augmentation scheme IV for a subject in the JAFFE database.

Augmentation Scheme V

This comprised the neutral expression faces of each subject, their left constructed faces (from scheme I), their right reconstructed faces (from scheme II) and the resulting images from Scheme IV. Thus, there were eight (8) images per subject available for training under this augmentation scheme.

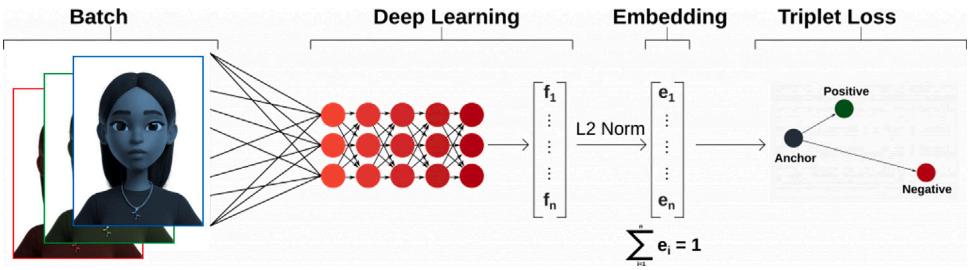

Fig. 7. FaceNet architecture.

Augmentation Scheme VI

This scheme comprised 18 images per subject for training the study algorithm. These images comprised the 8 images per subject as in scheme V and 10 additional images per subject obtained by using the transformations in scheme IV (slight rotations, horizontal flipping, shearing, brightness adjustments, and stretching) on the left and right reconstructed faces.

Feature extraction — FaceNet

Feature extractors or extraction techniques aim to find discriminative features from each face image for the purposes of matching against those of other faces to find a correct match. The FaceNet model aims to generate highly discriminative embeddings for faces, enabling accurate face identification and verification. It is a pre-trained deep convolutional neural network model which performs facial recognition using only 128 bytes per face [30]. According to William et al. [50], FaceNet is a method that uses deep convolutional networks to optimize its embedding, compared to using intermediate bottleneck layers as a test of previous deep learning approaches. They further described FaceNet as a one-shot learning method using Euclidean space to calculate the similarity distance for each face.

The FaceNet model learns a mapping function that directly maps input face images into a high-dimensional Euclidean space, where the distances between the embeddings of different faces reflect their similarity or dissimilarity [25]. This is achieved through a deep convolutional neural network (CNN) architecture that employs the inception module, enabling the model to capture features at different scales. During training, FaceNet uses a triplet loss function, which encourages the embeddings of matching faces to be closer in distance than those of non-matching faces. This facilitates the learning of highly discriminative features that are robust to variations in lighting conditions, poses, and other facial attributes [25]. FaceNet has demonstrated exceptional performance on popular face recognition benchmarks including, Labeled Faces in the Wild [51] and MegaFace [52]. The model has achieved state-of-the-art accuracy and outperforms previous approaches in various face recognition tasks. One of the significant advantages of FaceNet is its ability to generalize well across different datasets and domains, exhibiting robust performance even in the presence of large variations in facial appearance. Fig. 7 shows the FaceNet architecture.

Triplet loss

The triplet-based loss function is an adaptation of Kilian Weinberger's Large Margin Nearest Neighbor (LMNN) classifier for deep neural networks. Simply, the LMNN classifier continuously pulls together images of the same person and pushes away images of any other person.

Triplet loss training methods have three main elements namely anchor, positive and negative. The triplet loss works by minimizing the distance between anchors positively and maximizing the distance between anchors negatively. Where this positive has the same identity as the anchor and negative has a different identity from the anchor [50].

The process of training involves computing two Euclidean distances, say E_1 and E_2, between the anchor and the positive image and between the anchor and the negative image, respectively. The purpose of the training procedure is to reduce E_1 and increase E_2 as much as possible. This will lead to the formation of an embedding space in which images that are similar to one another will be located close to one another, while images that are vastly different will be located far apart. Fig. 8 shows the learning process using the triplet-based loss function.

Classification

The classification stage is the last stage in the face recognition process. In this stage, the facial embeddings created from the train images are matched against those from a test image using a classifier. In this regard, the study assessed the relative gains in recognition rates using three different classifiers.

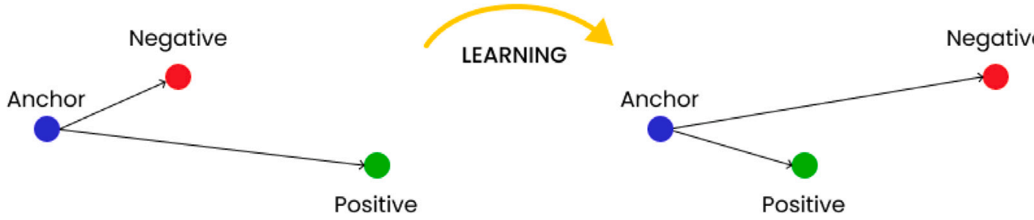

Fig. 8. Triplet loss — Learning process.

Support Vector Machine (SVM)

The SVM has been used for nonlinear classification, regression as well as outlier detection [53]. It uses a linear separating hyperplane to create a classifier with maximal margins [54].

For a given set of data which belongs to multiple classes, the Support Vector Machine classifier finds a hyperplane termed as the optimal separating hyperplane (OSH) that maximizes the distance from each class to the hyperplane. The hyperplane helps to classify or determine the most likely label for a new data.

Pisner and Schnyer [55] assert that the popularity of Support Vector Machine in classification problems is based on the fact that it is relatively simple and flexible. They further contend that SVMs typically provide a balanced predictive performance even in situations with limited sample sizes as well as being highly versatile across different data science scenarios. This assertion is also corroborated by Tian et al. [56], who state that SVMs have attractive properties such as good mathematical representations, strong generalization abilities as well as bright empirical performance. Application areas of SVMs include information security [57], speech recognition [58], and face verification and recognition [59].

Euclidean distance

The Euclidean distance-based classifier is widely recognized for its excellent discriminant performance when dealing with high-dimensional data [60]. In the context of image retrieval systems, Euclidean distance is used to determine the similarities between two pair of images. Some applications of Euclidean distance include performance comparison of distance matrices in content-based retrieval applications, and Photovoltaic single-diode model parameterization. As an application to calculus, Euclidean distance was applied to an I–V curve [61] and Rough IPFCM Clustering Algorithm and its Application on Smart Phones with Euclidean Distance [62].

City block

The City block distance, which is also known as the Manhattan distance, measures the sum of the absolute difference between two vectors. The City-Block Classifier is a supervised machine learning algorithm. Vargas et al. [17] also defines this classifier as an algorithm that examines the absolute difference between two objects. Some applications of City Block distance include Graphical Based Authentication Method Combined with City Block Distance for Electronic Payment Systems, Pain Detection in Biophysiological Signals: Knowledge Transfer from Short-Term to Long-Term Stimuli Based on Distance-Specific Segment Selection [20] and City Block Distance for Identification of Co-expressed MicroRNAs.

Results and discussion

We present the results of assessing the performance of FaceNet model when the test faces are characterized by moderately high occlusions (30% and 40% missingness), when statistical multiple imputation techniques (MICE, MissForest, RegEM) are used for occlusion recovery and under various augmentations of the single-image per person.

Assessment of the performance of FaceNet subject to occlusions and expressions on reconstructed faces

Table 1 shows the recognition rates of the FaceNet model under occlusion and expression variant constraints using the Support Vector Machines (SVM), Euclidean Distance (EUC) and City Block (CB) as classifiers. From Table 1, it can be seen that regardless of the classifier, the recognition rates were below 40% when the expression variant test faces were occluded at 30% and 40% rates. This performance is abysmally poor as it depicts that more than half of the images in the test-image database were wrongly matched by the FaceNet algorithm. The presence of higher levels of occlusions and varying expressions (multiple constraints) might have eroded significant facial features, thus, affecting the facial embeddings obtained by the FaceNet model.

From Table 2, the relative merit of using different statistical multiple schemes for occlusion recovery becomes more apparent. Particularly, the recognition rates associated with using all three imputation schemes are higher compared with recognition rates presented in Table 1. It is worthy to note that the highest recognition rates were obtained at both 30% and 40% reconstruction

Table 1
Recognition rates of FaceNet algorithm subject to occlusions and expressions constraints across the adopted classifiers.

Occlusion rate	SVM	EUC	CB
30%	31.48%	36.58%	36.57%
40%	21.67%	25.0%	25.0%

Table 2
Recognition rates of FaceNet algorithm on expression variant face images after de-occlusion.

Occlusion rate	De-Occlusion method	SVM	EUC	CB
30%	MICE	63.42%	81.48%	80.84%
	MissForest	64.81%	83.33%	83.80%
	RegEM	63.43%	81.48%	81.94%
40%	MICE	58.79%	73.61%	74.08%
	MissForest	62.80%	79.52%	78.59%
	RegEM	51.85%	67.60%	67.60%

Table 3
Performance of the FaceNet algorithm subject to augmentation scheme I (left half reconstructed faces) after de-occlusion.

Occlusion rate	De-Occlusion method	SVM	EUC	CB
30%	MICE	50.91%	81.94%	81.94%
	MissForest	51.35%	83.79%	83.79%
	RegEM	54.74%	81.48%	81.48%
40%	MICE	46.76%	74.07%	74.53%
	MissForest	51.33%	79.06%	78.15%
	RegEM	45.81%	76.29%	70.36%

rates (83.8% and 79.52% with City block and Euclidean distance classifiers respectively) using the MissForest imputation scheme, with the SVM classifier attaining the least marginal gains. This could be attributable to the limited number of images available for training the FaceNet model. Specifically, using MICE imputation mechanism, the FaceNet algorithm recorded its highest average recognition rates of 80.84% and 74.08% at 30% and 40% occlusion rates respectively through the City block classifier. Also, using the RegEM de-occlusion mechanism, the FaceNet algorithm recorded its highest average recognition rates of 81.94% and 67.60% at 30% and 40% occlusion rates through the City block and Euclidean distance classifiers respectively.

Assessing the effects of train-image data augmentation on the performance of the FaceNet model

Augmentation schemes help provide adequate data or information on the subjects in the study database to aid the recognition process. They present the recognition module with several image acquisition possibilities relevant for training. That is, sufficient information on subjects in the study database are provided for training of the FaceNet recognition algorithm. These also help to prevent overfitting of the recognition module.

The study employed six (6) train-image data augmentation schemes aimed at enhancing the performance of the FaceNet model and the results are presented in Tables 3–8.

From Table 3, it can be seen that augmenting the neutral train images of subjects with their left reconstructed images obtained from their half segmented faces (Scheme I) resulted in a moderate increase in recognition rate particularly for the MICE imputation mechanism. Specifically, using the MICE imputation mechanism, the performance of the FaceNet algorithm increase from its highest of 81.48% (with Euclidean distance classifier) and 74.08% (with City block classifier) for 30% and 40% occlusion rates in Table 2 to 81.94% (with City block classifier) and 74.53% (with City block classifier) respectively under augmentation scheme I. It is also evident from Tables 2 and 3 that the performance of the FaceNet algorithm recorded some marginal decline using the Missforest and RegEM de-occlusion mechanism under augmentation scheme I (left half reconstructed face).

From Table 4, the performance of the FaceNet model when the single train images of subjects were augmented with their right reconstructed faces (Scheme II) was lower relative to the use of the left reconstructed face. Specifically, the performance of the FaceNet model declined from its highest of; 83.80% to 82.87% (using Missforest at 30% occlusion rate), 81.48% to 79.63% (using MICE at 30% occlusion rate) except for RegEM at 30% occlusion rate which increased from 81.94% to 82.41%. Similar trend can be observed from Tables 2 and 4 for the 40% occlusion rate. This result is consistent with [32,63] who explored the bilateral symmetry property of the human face in face recognition. They found that, recognition algorithms have relatively higher average recognition rates and lower average recognition distances when left half reconstructed face images are used as test images for recognition.

A noticeable result from Table 5 is the increase in performance of the FaceNet model using the SVM for classification when both left and right reconstructed faces were used to augment the neutral face images of each subjects for training, although the recognition rates attained were significantly lower compared with the use of Euclidean distance (EUC) and City Block (CB) classifiers. The average recognition rates of FaceNet algorithm using the RegEM de-occlusion mechanism increased slightly its highest of 81.94%

Table 4
Performance of the FaceNet algorithm subject to augmentation scheme II (right half reconstructed faces) after de-occlusion.

Occlusion rate	De-Occlusion method	SVM	EUC	CB
30%	MICE	48.61%	79.63%	79.11%
	MissForest	53.24%	82.87%	82.39%
	RegEM	54.17%	81.48%	82.41%
40%	MICE	46.76%	72.22%	72.22%
	MissForest	48.84%	78.59%	77.66%
	RegEM	44.44%	67.59%	66.21%

Table 5
Performance of the FaceNet algorithm subject to augmentation scheme III (left and right reconstructed faces) after de-occlusion.

Occlusion rate	De-Occlusion method	SVM	EUC	CB
30%	MICE	69.91%	80.55%	80.47%
	MissForest	69.45%	83.80%	83.34%
	RegEM	66.66%	81.48%	81.95%
40%	MICE	58.79%	73.15%	74.08%
	MissForest	68.37%	78.12%	77.20%
	RegEM	54.17%	70.37%	69.91%

Table 6
Performance of the FaceNet algorithm subject to augmentation scheme IV after de-occlusion.

Occlusion rate	De-Occlusion method	SVM	EUC	CB
30%	MICE	83.33%	82.41%	81.48%
	MissForest	85.19%	84.26%	85.19%
	RegEM	81.95%	82.40%	82.87%
40%	MICE	74.04%	73.61%	74.07%
	MissForest	79.52%	78.13%	79.52%
	RegEM	70.37%	66.66%	68.06%

to 81.95% (at 30% occlusion rate) and 67.60% to 70.37% (at 40% occlusion rate). The use of both left and right reconstructed images in augmentation scheme III provides more information on the subjects in the recognition module. This could account for the marginal increase in the average recognition rates with the SVM classifier. It is also evident from Tables 2 and 5 that, the effect of the augmentation scheme III on the performance of FaceNet module is not too appreciable except for the marginal gains using the SVM classifier.

The performance of the FaceNet model subject to augmentation scheme IV is presented in Table 6. It is seen that this augmentation scheme sufficed to enhance greatly the performance of the FaceNet model with SVM and CB classifiers, using the MissForest imputation scheme for occlusion recovery. Specifically, the average recognition rates of the FaceNet algorithm increased from its highest in Table 2 of; 81.48% to 83.33% (using MICE at 30% occlusion rate), 83.80% to 85.19% (using Missforest at 30% occlusion rate) and 81.94% to 82.87% (using RegEM at 30% occlusion rate) whereas at 40% occlusion rate, the performance of the FaceNet model remained somewhat stable in Table 6. Generally, the augmentation schemes help provide adequate data or information on the subjects in study database to aid the recognition process. The performance of the recognition algorithms tends to improves as the data in the augmentation schemes increase. This is evident from the findings in Tables 3–6 on augmentation schemes I, II, III and IV and very obvious using the SVM classifier.

From Tables 7 and 8, there were marginal differences in average recognition rates under augmentation schemes V and VI, across all imputation mechanisms (MICE, Missforest and RegEM) and classifiers (SVM, EU and CB). This suggests some level of saturation in reference to availability of training samples for the model.

In effect, among all the six train-image data augmentation schemes considered, augmentation scheme IV (applying various transformations, including slight rotations, horizontal flipping, shearing, brightness adjustments, and stretching) resulted in the highest recognition rates (85.19% and 79.52%) of FaceNet model at 30% and 40% occlusion rates using MissForest occlusion recovery respectively and corresponded to the choice of SVM or CB for classification. Under this augmentation scheme, the average run-time for the FaceNet algorithm in recognition of an image in the test database was about 0.98 s (less than 1 s).

Comparison of the performance of the FaceNet model with some PCA-based algorithms

Table 9 presents the average recognition rates using PCA-based algorithms following different preprocessing mechanisms (Discrete Cosine Transform (DCT) or Histogram Equalization and Discrete Wavelet Transform (HE-DWT) or Discrete Wavelet Transform (DWT)) and the City Block distance for classification. It worthy to note that the MICE, MissForest and RegEM imputation

Table 7
Performance of the FaceNet algorithm subject to augmentation scheme V after de-occlusion.

Occlusion rate	Method	SVM	EUC	CB
30%	MICE	81.95%	81.95%	81.02%
	MissForest	84.52%	83.80%	83.34%
	RegEM	81.49%	81.49%	81.02%
40%	MICE	71.76%	73.15%	74.54%
	MissForest	77.67%	76.74%	76.27%
	RegEM	69.44%	67.13%	67.96%

Table 8
Performance of the FaceNet algorithm subject to augmentation scheme VI after de-occlusion.

Occlusion rate	Method	SVM	EUC	CB
30%	MICE	82.87%	81.95%	81.48%
	MissForest	82.41%	83.80%	83.80%
	RegEM	80.55%	82.87%	82.41%
40%	MICE	72.22%	75.46%	74.54%
	MissForest	77.66%	77.66%	78.59%
	RegEM	68.06%	68.06%	68.06%

Table 9
Performance of PCA algorithms on reconstructed faces.

Occlusion rate	Method	HE-DWT-PCA	DWT-PCA	DCT-PCA
30%	MICE	75.93%	55.09%	72.69%
	MissForest	76.85%	47.69%	78.24%
	RegEM	68.98%	59.26%	73.61%
40%	MICE	70.37%	26.85%	58.33%
	MissForest	67.81%	39.81%	64.81%
	RegEM	57.41%	42.59%	61.57%

mechanisms were used to reconstruct the occluded face images (30% and 40% occlusion levels) before passing them into the PCA-based face recognition module recognition. It can be observed that the choice of preprocessing mechanism (HE-DWT, DWT or DCT) also impacted significantly on the recognition rates attained with the use of the different preprocessed reconstructed faces as test faces.

The DCT-PCA algorithm recorded the highest average recognition rate (78.24%) at 30% occlusion rate using Missforest imputation mechanism for reconstruction/de-occlusion and HE-DWT-PCA algorithm has the highest average recognition rate (70.37%) at 40% occlusion rate using MICE imputation mechanism for reconstruction/de-occlusion. Although the PCA-based methods have lower computational complexities and runtimes, the FaceNet algorithm subject augmentation scheme IV out-performed the enhanced PCA-based methods at both 30% and 40% occlusion rates, recording relatively higher average recognition rates of 85.19% and 79.52% respectively.

Conclusions and recommendations

The study sought to investigate the performance of the FaceNet face recognition model when test faces are acquired under multiple constraints (moderately high occlusions and varying expressions) and the effect of using statistical multiple imputation techniques to solve the occlusion challenge. 128-D FaceNet's facial embeddings were generated for face images and their similarities were subsequently attained using three classifiers (SVM, Euclidean distance, and City Block). It can be concluded from the results of the study that;

- the presence of multiple constraints greatly affected the performance of the FaceNet model at both 30% and 40% occlusion rates. This can be attributed to the presence of occlusions degraded critical facial components, affecting the embeddings created by using FaceNet for feature representations. These findings underscore the effect of poor image quality on the performance of face recognition algorithms [64,65] and suggest the need for corrective mechanisms.
- the use of the three multiple imputation-based (MICE, MissForest, and RegEM) test faces for recognition enhanced the performance of the FaceNet model relative to that of the occluded expression variant faces, affirming the relative effectiveness of using some statistical imputation methods in dealing with occlusions as noted in [14,66]. Particularly, the findings of the study showed that MissForest imputation methods could be harnessed for addressing occlusion-related challenges in face images when FaceNet embeddings are sought for face representation.
- the FaceNet model outperformed some existing enhanced PCA-based algorithms recording relatively higher average recognition rates of 85.19% and 79.5% at 30% and 40% occlusion levels respectively.

- the performance of the FaceNet model could be further enhanced in using data augmentation schemes. Particularly for this study, the augmentation scheme IV (slight rotations, horizontal flipping, shearing, brightness adjustments, and stretching) was found as the most suitable scheme for training of the FaceNet recognition module.

Overall, the study highlighted the importance of carefully considering the choice of classifier, as its inherent characteristics can impact the gains derived from the use of statistical imputation-based approaches in face recognition systems. These findings provide valuable insights into the potential use of statistical multiple imputation methods in multiple constrained face recognition problems, particularly with deep learning face recognition algorithms. The study therefore recommends the MissForest multiple imputation method as an occlusion recovery technique as well as data augmentation for performance enhancement when there are limited images per subject for training. The proposed deep learning module can be applied in health science for the detection of defective organs and for the recognition of foreign objects in the human body using X-ray images. In Agriculture, it can be used to detect diseased plants using images of parts of the plants (leaves, stem, branches etc.). It can also be applied to fingerprint and iris recognitions.

As shown by William et al. [50], the training process of the FaceNet algorithm requires complex computing and a long computational time. By integrating the Tensorflow learning machine and pre-trained model, they achieved a relatively shorter training time with similar computational complexity. In this study, the recommended FaceNet algorithm under imputation scheme IV gave an average run-time of 0.98 s per image. This is relatively high as compared to the run-time of most PCA-based techniques in Literature. As shown in Table 9, the performance of the enhanced PCA-based methods is still hindered by higher levels of occlusions and varying expressions. Future works would focus on enhancing the PCA-based methods which has been shown to have lower computation complexity and shorter run-time to adequately recognize expression variant face images with higher levels of occlusions.

CRediT authorship contribution statement

Joseph A. Mensah: Conceptualization, Methodology, Writing – original draft. **Justice K. Appati:** Data curation, Formal analysis. **Elijah K.A Boateng:** Data curation, Formal analysis. **Eric Ocran:** Data curation, Formal analysis. **Louis Asiedu:** Supervision, Validation, Writing – review & editing.

Declaration of competing interest

The authors declare that they have no known competing financial interests or personal relationships that could have appeared to influence the work reported in this paper.

Data availability

The data used to support the findings of this study are available from the corresponding author upon request.

References

[1] P. Li, L. Prieto, D. Mery, P. Flynn, Face recognition in low quality images: A survey, 2018, arXiv preprint arXiv:1805.11519.
[2] S. Anwarul, S. Dahiya, A comprehensive review on face recognition methods and factors affecting facial recognition accuracy, in: Proceedings of ICRIC 2019: Recent Innovations in Computing, Springer, 2020, pp. 495–514.
[3] Y. Cheon, D. Kim, Natural facial expression recognition using differential-AAM and manifold learning, Pattern Recognit. 42 (7) (2009) 1340–1350.
[4] X. Deng, F. Da, H. Shao, Y. Jiang, A multi-scale three-dimensional face recognition approach with sparse representation-based classifier and fusion of local covariance descriptors, Comput. Electr. Eng. 85 (2020) 106700.
[5] D. Goren, H.R. Wilson, Quantifying facial expression recognition across viewing conditions, Vis. Res. 46 (8–9) (2006) 1253–1262.
[6] N. Alyüz, B. Gökberk, L. Spreeuwers, R. Veldhuis, L. Akarun, Robust 3D face recognition in the presence of realistic occlusions, in: 2012 5th IAPR International Conference on Biometrics (ICB), IEEE, 2012, pp. 111–118.
[7] B. Lahasan, S.L. Lutfi, R. San-Segundo, A survey on techniques to handle face recognition challenges: occlusion, single sample per subject and expression, Artif. Intell. Rev. 52 (2019) 949–979.
[8] R. Min, A. Hadid, J.-L. Dugelay, et al., Efficient detection of occlusion prior to robust face recognition, Sci. World J. 2014 (2014).
[9] C.D. Pain, G.F. Egan, Z. Chen, Deep learning-based image reconstruction and post-processing methods in positron emission tomography for low-dose imaging and resolution enhancement, Eur. J. Nucl. Med. Mol. Imaging 49 (9) (2022) 3098–3118.
[10] I. Tabian, H. Fu, Z. Sharif Khodaei, A convolutional neural network for impact detection and characterization of complex composite structures, Sensors 19 (22) (2019) 4933.
[11] J.A. Fessler, Model-based image reconstruction for MRI, IEEE Signal Process. Mag. 27 (4) (2010) 81–89.
[12] L. Liu, Model-based iterative reconstruction: a promising algorithm for today's computed tomography imaging, J. Med. Imaging Radiat. Sci. 45 (2) (2014) 131–136.
[13] W. Chang, J.M. Lee, K. Lee, J.H. Yoon, M.H. Yu, J.K. Han, B.I. Choi, Assessment of a model-based, iterative reconstruction algorithm (MBIR) regarding image quality and dose reduction in liver computed tomography, Invest. Radiol. 48 (8) (2013) 598–606.
[14] L. Asiedu, J.A. Mensah, F. Ayiah-Mensah, F.O. Mettle, Assessing the effect of data augmentation on occluded frontal faces using DWT-PCA/SVD recognition algorithm, Adv. Multimed. 2021 (2021) 1–11.
[15] I.L. Animasaun, N.A. Shah, A. Wakif, B. Mahanthesh, R. Sivaraj, O.K. Koríko, Ratio of Momentum Diffusivity to Thermal Diffusivity: Introduction, Meta-Analysis, and Scrutinization, CRC Press, 2022.
[16] P.P. Shinde, S. Shah, A review of machine learning and deep learning applications, in: 2018 Fourth International Conference on Computing Communication Control and Automation (ICCUBEA), IEEE, 2018, pp. 1–6.
[17] R. Vargas, A. Mosavi, R. Ruiz, Deep learning: a review, 2017.

[18] H. Chen, Y. Wang, T. Guo, C. Xu, Y. Deng, Z. Liu, S. Ma, C. Xu, C. Xu, W. Gao, Pre-trained image processing transformer, in: Proceedings of the IEEE/CVF Conference on Computer Vision and Pattern Recognition, 2021, pp. 12299–12310.

[19] F. Wang, L.P. Casalino, D. Khullar, Deep learning in medicine– promise, progress, and challenges, JAMA Internal Med. 179 (3) (2019) 293–294.

[20] F. Piccialli, V. Di Somma, F. Giampaolo, S. Cuomo, G. Fortino, A survey on deep learning in medicine: Why, how and when? Inf. Fusion 66 (2021) 111–137.

[21] O.N. Oyelade, A.E. Ezugwu, Characterization of abnormalities in breast cancer images using nature-inspired metaheuristic optimized convolutional neural networks model, Concurr. Comput.: Pract. Exper. 34 (4) (2022) e6629.

[22] R. Josphineleela, P. Raja Rao, A. Shaikh, K. Sudhakar, A multi-stage faster RCNN-based isplinception for skin disease classification using novel optimization, J. Digit. Imaging (2023) 1–17.

[23] K. Sundararajan, D.L. Woodard, Deep learning for biometrics: A survey, ACM Comput. Surv. 51 (3) (2018) 1–34.

[24] M. Wu, L. Chen, Image recognition based on deep learning, in: 2015 Chinese Automation Congress (CAC), IEEE, 2015, pp. 542–546.

[25] F. Schroff, D. Kalenichenko, J. Philbin, Facenet: A unified embedding for face recognition and clustering, in: Proceedings of the IEEE Conference on Computer Vision and Pattern Recognition, 2015, pp. 815–823.

[26] J. Brownlee, How to develop a face recognition system using FaceNet in keras, Mach. Learn. Mastery 21 (2019).

[27] L.Q. Vu, P.T. Trieu, H.-S. Nguyen, Implementation of FaceNet and support vector machine in a real-time web-based timekeeping application, IAES Int. J. Artif. Intell. 11 (1) (2022) 388.

[28] F.D. Adhinata, D.P. Rakhmadani, D. Wijayanto, Fatigue detection on face image using FaceNet algorithm and K-nearest neighbor classifier, J. Inf. Syst. Eng. Bus. Intell. 7 (1) (2021) 22–30.

[29] F.D. Adhinata, N.A.F. Tanjung, W. Widayat, G.R. Pasfica, F.R. Satura, Real-time masked face recognition using FaceNet and supervised machine learning, in: Proceedings of the 2nd International Conference on Electronics, Biomedical Engineering, and Health Informatics: ICEBEHI 2021, 3–4 November, Surabaya, Indonesia, Springer, 2022, pp. 189–202.

[30] M.R. Golla, P. Sharma, Performance evaluation of facenet on low resolution face images, in: Communication, Networks and Computing: First International Conference, CNC 2018, Gwalior, India, March 22-24, 2018, Revised Selected Papers 1, Springer, 2019, pp. 317–325.

[31] A.C. Bovik, Handbook of Image and Video Processing, Academic Press, 2010.

[32] L. Asiedu, F.O. Mettle, J.A. Mensah, Recognition of reconstructed frontal face images using fft-pca/svd algorithm, J. Appl. Math. 2020 (2020) 1–8.

[33] G.H. Golub, M. Heath, G. Wahba, Generalized cross-validation as a method for choosing a good ridge parameter, Technometrics 21 (2) (1979) 215–223.

[34] Y. Liu, S.D. Brown, Comparison of five iterative imputation methods for multivariate classification, Chemometr. Intell. Lab. Syst. 120 (2013) 106–115.

[35] T.D. Le, R. Beuran, Y. Tan, Comparison of the most influential missing data imputation algorithms for healthcare, in: 2018 10th International Conference on Knowledge and Systems Engineering (KSE), IEEE, 2018, pp. 247–251.

[36] F. Liang, B. Jia, J. Xue, Q. Li, Y. Luo, An imputation–regularized optimization algorithm for high dimensional missing data problems and beyond, J. R. Stat. Soc. Ser. B Stat. Methodol. 80 (5) (2018) 899–926.

[37] X. Liu, X. Wang, L. Zou, J. Xia, W. Pang, Spatial imputation for air pollutants data sets via low rank matrix completion algorithm, Environ. Int. 139 (2020) 105713.

[38] E. Slade, M.G. Naylor, A fair comparison of tree-based and parametric methods in multiple imputation by chained equations, Stat. Med. 39 (8) (2020) 1156–1166.

[39] G. Chhabra, V. Vashisht, J. Ranjan, A comparison of multiple imputation methods for data with missing values, Indian J. Sci. Technol. 10 (19) (2017) 1–7.

[40] Y. Deng, C. Chang, M.S. Ido, Q. Long, Multiple imputation for general missing data patterns in the presence of high-dimensional data, Sci. Rep. 6 (1) (2016) 21689.

[41] M. Resche-Rigon, I.R. White, J.W. Bartlett, S.A. Peters, S.G. Thompson, P.-I.S. Group, Multiple imputation for handling systematically missing confounders in meta-analysis of individual participant data, Stat. Med. 32 (28) (2013) 4890–4905.

[42] R.A. Hughes, I.R. White, S.R. Seaman, J.R. Carpenter, K. Tilling, J.A. Sterne, Joint modelling rationale for chained equations, BMC Med. Res. Methodol. 14 (2014) 1–10.

[43] M. Resche-Rigon, I.R. White, Multiple imputation by chained equations for systematically and sporadically missing multilevel data, Stat. Methods Med. Res. 27 (6) (2018) 1634–1649.

[44] S. Hong, H.S. Lynn, Accuracy of random-forest-based imputation of missing data in the presence of non-normality, non-linearity, and interaction, BMC Med. Res. Methodol. 20 (1) (2020) 1–12.

[45] D.J. Stekhoven, P. Bühlmann, MissForest– non-parametric missing value imputation for mixed-type data, Bioinformatics 28 (1) (2012) 112–118.

[46] A.K. Waljee, A. Mukherjee, A.G. Singal, Y. Zhang, J. Warren, U. Balis, J. Marrero, J. Zhu, P.D. Higgins, Comparison of imputation methods for missing laboratory data in medicine, BMJ Open 3 (8) (2013) e002847.

[47] N. Solaro, A. Barbiero, G. Manzi, P. Ferrari, A simulation comparison of imputation methods for quantitative data in the presence of multiple data patterns, J. Stat. Comput. Simul. 88 (18) (2018) 3588–3619.

[48] A.D. Shah, J.W. Bartlett, J. Carpenter, O. Nicholas, H. Hemingway, Comparison of random forest and parametric imputation models for imputing missing data using MICE: a CALIBER study, Am. J. Epidemiol. 179 (6) (2014) 764–774.

[49] C. Shorten, T.M. Khoshgoftaar, A survey on image data augmentation for deep learning, J. Big Data 6 (1) (2019) 1–48.

[50] I. William, E.H. Rachmawanto, H.A. Santoso, C.A. Sari, et al., Face recognition using facenet (survey, performance test, and comparison), in: 2019 Fourth International Conference on Informatics and Computing (ICIC), IEEE, 2019, pp. 1–6.

[51] G.B. Huang, M. Mattar, T. Berg, E. Learned-Miller, Labeled faces in the wild: A database forstudying face recognition in unconstrained environments, in: Workshop on Faces in'Real-Life'Images: Detection, Alignment, and Recognition, 2008.

[52] I. Kemelmacher-Shlizerman, S.M. Seitz, D. Miller, E. Brossard, The megaface benchmark: 1 million faces for recognition at scale, in: Proceedings of the IEEE Conference on Computer Vision and Pattern Recognition, 2016, pp. 4873–4882.

[53] A. Mammone, M. Turchi, N. Cristianini, Support vector machines, Wiley Interdiscip. Rev. Comput. Stat. 1 (3) (2009) 283–289.

[54] L. Wang, Support Vector Machines: Theory and Applications, Vol. 177, Springer Science & Business Media, 2005.

[55] D.A. Pisner, D.M. Schnyer, Support vector machine, in: Machine Learning, Elsevier, 2020, pp. 101–121.

[56] Y. Tian, Y. Shi, X. Liu, Recent advances on support vector machines research, Technol. Econ. Dev. Econ. 18 (1) (2012) 5–33.

[57] S. Mukkamala, G. Janoski, A. Sung, Intrusion detection using neural networks and support vector machines, in: Proceedings of the 2002 International Joint Conference on Neural Networks. IJCNN'02 (Cat. No. 02CH37290), Vol. 2, IEEE, 2002, pp. 1702–1707.

[58] A. Ganapathiraju, J.E. Hamaker, J. Picone, Applications of support vector machines to speech recognition, IEEE Trans. Signal Process. 52 (8) (2004) 2348–2355.

[59] K. Jonsson, J. Kittler, Y. Li, J. Matas, Support vector machines for face authentication, Image Vis. Comput. 20 (5–6) (2002) 369–375.

[60] T. Nakagawa, S. Ohtsuka, An asymptotic expansion for the distribution of euclidean distance-based discriminant function in normal populations, J. Stat. Theory Pract. 16 (4) (2022) 62.

[61] V. Galiano, F.J. Toledo, J.M. Blanes, V. Herranz, E. Batzelis, Photovoltaic single-diode model parametrization. An application to the calculus of the euclidean distance to an IV curve, 2022.

[62] C.-M. Chen, S.-C. Chang, C.-C. Chuang, J.-T. Jeng, Rough IPFCM clustering algorithm and its application on smart phones with euclidean distance, Appl. Sci. 12 (10) (2022) 5195.

[63] A.K. Singh, G.C. Nandi, Face recognition using facial symmetry, in: Proceedings of the Second International Conference on Computational Science, Engineering and Information Technology, 2012, pp. 550–554.

[64] D. Zeng, R. Veldhuis, L. Spreeuwers, A survey of face recognition techniques under occlusion, IET Biom. 10 (6) (2021) 581–606.

[65] J.A. Mensah, L. Asiedu, F.O. Mettle, S. Iddi, Assessing the performance of DWT-PCA/SVD face recognition algorithm under multiple constraints, J. Appl. Math. 2021 (2021) 1–12.

[66] F. Ayiah-Mensah, L. Asiedu, F.O. Mettle, R. Minkah, Recognition of augmented frontal face images using FFT-PCA/SVD algorithm, Appl. Comput. Intell. Soft Comput. 2021 (2021) 1–9.